

Photochemical Ligand Substitution Reactions of *fac*-[Re(bpy)(CO)₃Cl] and DerivativesShunsuke Sato,[†] Akiko Sekine,[†] Yuji Ohashi,[†] Osamu Ishitani,^{*,†} Ana Maria Blanco-Rodríguez,^{||} Antonín Vlček, Jr.,^{||} Taiju Unno,[‡] and Kazuhide Koike[§]

Department of Chemistry and Department of Chemistry and Materials Science, Graduate School of Science and Engineering, Tokyo Institute of Technology, O-okayama 2-12-1, E1-9, Meguro-ku, Tokyo 152-8551, Japan, National Institute of Advanced Industrial Science and Technology, Onogawa 16-1, Tsukuba 305-8569, Japan, and School of Biological and Chemical Sciences, Queen Mary, University of London, Mile End Road, London E1 4NS, U.K.

Received November 14, 2006

Excitation by high-energy light, such as that of 313 nm wavelength, induces a photochemical ligand substitution (PLS) reaction of *fac*-[Re(bpy)(CO)₃Cl] (**1a**) to give the solvento complexes (OC-6-34)- and (OC-6-44)-[Re(bpy)(CO)₂(MeCN)Cl] (**2** and **3**) in good yields. The disappearance quantum yield of **1a** was 0.01 ± 0.001 at 313 nm. The products were isolated, and X-ray crystallographic analysis was successfully performed for **2**. Time-resolved IR measurements clearly indicated that the CO ligand dissociates with subpicosecond rates after excitation, leading to vibrationally hot photoproducts, which relax within 50–100 ps. Detailed studies of the reaction mechanism show that the PLS reaction of **1a** does not proceed via the lowest vibrational level in the ³MLCT excited state. The PLS reaction gives **2** and (OC-6-24)-[Re(bpy)(CO)₂(MeCN)Cl] (**5**) as primary products, and one of the products, **5**, isomerizes to **3**. This type of PLS reaction is more general, occurring in various *fac*-rhenium(I) diimine tricarbonyl complexes such as *fac*-[Re(X₂bpy)(CO)₃Cl] (X₂bpy = 4,4'-X₂-bpy; X = MeO, NH₂, CF₃), *fac*-[Re(bpy)(CO)₃(pyridine)]⁺, and *fac*-[Re(bpy)(CO)₃(MeCN)]⁺. The stable photoproducts (OC-6-44)- and (OC-6-43)-[Re(bpy)(CO)₂(MeCN)(pyridine)]⁺ and (OC-6-32)- and (OC-6-33)-[Re(bpy)(CO)₂(MeCN)₂]⁺ were isolated. The PLS reaction of rhenium tricarbonyl–diimine complexes is therefore applicable as a general synthetic method for novel dicarbonyls.

Introduction

The photochemical and photophysical properties of rhenium(I) diimine tricarbonyl complexes have now attracted a great deal of attention for three decades.¹ The complexes have been used as an efficient photocatalyst for CO₂ reduction,² a building block for emissive supramolecules,³ an emitter for electroluminescence devices,⁴ and a light absorber for Grätzel-type solar cells.⁵ The chloro complex *fac*-[Re(bpy)(CO)₃Cl] (**1a**) and its derivatives have been studied in great detail.^{1,6–8} It is well-established that emission,

energy transfer, and electron transfer occur mainly from the lowest vibrational level of the triplet metal-to-ligand-charge-transfer (³MLCT) excited state or from the triplet ligand-

* To whom correspondence should be addressed. E-mail: ishitani@chem.titech.ac.jp.

[†] Tokyo Institute of Technology.

[‡] Saitama University.

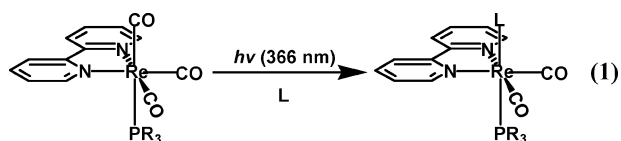
[§] National Institute of Advanced Industrial Science and Technology.

^{||} Queen Mary, University of London.

- (1) (a) Wrighton, M. S.; Morse, D. L. *J. Am. Chem. Soc.* **1974**, *96*, 998. (b) Luong, J. C.; Falynak, H.; Wrighton, M. S. *J. Am. Chem. Soc.* **1979**, *101*, 1597. (c) Giordano, P. J.; Wrighton, M. S. *J. Am. Chem. Soc.* **1979**, *101*, 2888. (d) Stufkens, D. J.; Vlček, A., Jr. *Coord. Chem. Rev.* **1998**, *177*, 127.

- (2) (a) Hawecker, J.; Lehn, J. M.; Ziessel, R. *Helv. Chim. Acta* **1986**, *69*, 1990. (b) Hori, H.; Johnson, F. P. A.; Koike, K.; Ishitani, O.; Ibusuki, T. *J. Photochem. Photobiol., A* **1996**, *96*, 171. (c) Koike, K.; Hori, H.; Ishizuka, M.; Westwell, J. R.; Takeuchi, K.; Ibusuki, T.; Enjouji, K.; Konno, H.; Sakamoto, K.; Ishitani, O. *Organometallics* **1997**, *16*, 5724. (d) Hori, H.; Ishihara, J.; Koike, K.; Takeuchi, K.; Ibusuki, T.; Ishitani, O. *J. Photochem. Photobiol., A* **1999**, *120*, 119. (e) Tsubaki, H.; Tohyama, S.; Koike, K.; Saitoh, H.; Ishitani, O. *J. Chem. Soc., Dalton Trans.* **2005**, 385. (f) Tsubaki, H.; Sekine, A.; Ohashi, Y.; Koike, K.; Takeda, H.; Ishitani, O. *J. Am. Chem. Soc.* **2005**, *127*, 15544.
- (3) (a) Belanger, S.; Hupp, J. T.; Stern, C. L.; Slone, R. V.; Watson, D. F.; Carrell, T. G. *J. Am. Chem. Soc.* **1999**, *121*, 557. (b) Sun, S. S.; Lees, A. J. *J. Am. Chem. Soc.* **2000**, *122*, 8956.
- (4) Yam, V. W. W.; Li, B.; Yang, Y.; Chu, B. W. K.; Wong, K. M. C.; Cheung, K. K. *Eur. J. Inorg. Chem.* **2003**, *22*, 4035.
- (5) (a) Hasselmann, G. M.; Meyer, G. J. *Z. Phys. Chem.* **1999**, *212*, 39. (b) Polo, A. S.; Itokazu, M. K.; Murakami Iha, N. Y. *Coord. Chem. Rev.* **2004**, *248*, 1343.
- (6) Caspar, J. V.; Meyer, T. J. *J. Phys. Chem.* **1983**, *87*, 952.
- (7) Worl, L. A.; Duesing, R.; Chen, P.; Ciana, L. D.; Meyer, T. J. *J. Chem. Soc., Dalton Trans.* **1991**, 849.

centered excited state.^{1,9–12} However, there has been no report of photochemical ligand substitution (PLS) reactions in these types of complexes. The chloride ligand can be thermally substituted with other ligands such as pyridine, acetonitrile, and phosphorus compounds by using a silver cation to give *fac*-[Re(bpy)(CO)₃(L)]⁺-type complexes in good yields. However, these had not been good methods for substitution of the three carbonyl ligands of the rhenium(I) diimine tricarbonyl complexes. We have recently reported PLS reactions of the complexes with a phosphorus ligand, *fac*-[Re(X₂bpy)(CO)₃(PR₃)]⁺,¹³ which efficiently occur using any wavelength light that can be absorbed by the complexes and selectively give *cis,trans*-[Re(X₂bpy)(CO)₂(PR₃)(L)]ⁿ⁺ (*n* = 0, L = Cl; *n* = 1, L = pyridine, acetonitrile, PR₃) as shown in eq 1.



Mechanistic studies clearly showed that this PLS reaction proceeds via the triplet metal-centered (³MC) excited state, which is in thermal equilibrium with the ³MLCT excited state. Because the rhenium(I) diimine dicarbonyl complexes have some interesting properties,^{13a} the development of general synthetic methods for such complexes has been desired. However, this type of photochemical reaction via a ³MC excited state occurs only in the cases of rhenium(I) diimine tricarbonyl complexes with a phosphorus ligand. Although similar PLS reactions of other metal carbonyls such as Cr, Mo, W, and Mn complexes have been reported,^{14–17} as mentioned above, there has been no report of PLS reactions of not only *fac*-[Re(bpy)(CO)₃Cl] but also *fac*-[Re(bpy)(CO)₃(L)]⁺ (L ≠ PR₃).

Scheme 1. Structures of the Isolated Rhenium(I) Dicarbonyl Complexes (OC-6-*m*)-[Re(bpy)(CO)₂(L)(L')]ⁿ⁺

cis,trans type complexes				cis,cis type complexes			
	m	L	L'		m	L	L'
2	34	Cl	MeCN	3	44	Cl	MeCN
8	44	pyridine	MeCN	4	44	P(OEt) ₃	MeCN
10	33	MeCN	MeCN	5	24	MeCN	Cl
				9	43	pyridine	MeCN
				11	32	MeCN	MeCN

We report here some relatively efficient PLS reactions of *fac*-[Re(X₂bpy)(CO)₃Cl] (X₂bpy = 4,4'-X₂bpy; X = H, OMe, NH₂, CF₃) and *fac*-[Re(bpy)(CO)₃(L)]⁺ (L = pyridine and MeCN) using high-energy UV light. The reactions proceed via a mechanism different from that of [Re(X₂bpy)(CO)₃(PR₃)]⁺ described above. New dicarbonyl rhenium(I) complexes, (OC-6-34)- and (OC-6-44)-[Re(bpy)(CO)₂(MeCN)Cl] (**2** and **3**), (OC-6-44)- and (OC-6-43)-[Re(bpy)(CO)₂(MeCN)-(pyridine)]⁺CF₃SO₃⁻ (**8** and **9**), and (OC-6-32)- and (OC-6-32)-[Re(bpy)(CO)₂(MeCN)₂]⁺ PF₆⁻ (**10** and **11**), were isolated (Scheme 1), and their spectroscopic and electrochemical properties and X-ray crystallographic data are also reported.

Experimental Section

General Procedures. High-performance liquid chromatography (HPLC) analyses were conducted using a Shimadzu LC-10ADVP pump with a Develosil ODS-UG-5 column (250 mm × 4.6 mm), a Rheodyne 7125 injector, a Shimadzu FCV-10ALVP gradient unit, and a Shimadzu SPD-10AVVP detector. The column temperature was kept at 303 K using a Shimadzu CTO-10ACVP oven. A 4:6 (v/v) mixture of MeOH and a KH₂PO₄–NaOH buffer (0.05 M, pH. 5.9) was used as the first eluent up to 20 min, and then the eluent was gradually changed to a 7:3 (v/v) mixture of MeOH and the KH₂PO₄–NaOH buffer for 5 min. ESI-MS analyses were performed using a Shimadzu LCMS-2010A system with HPLC-grade MeOH or MeOH/H₂O (4:6) as the eluent. IR spectra were recorded with a JEOL JIR-6500 FTIR spectrophotometer using 1 cm⁻¹ resolution. UV–vis spectra were measured with a Jasco V-565 or Photal MCPD-2000 spectrophotometer. Emission spectra were recorded at 25 ± 0.1 °C using a Jasco FP-6600 spectrofluorometer with correction for the detector sensitivity determined using correction data supplied by Jasco. All emission spectra were measured in acetonitrile solutions. Emission quantum yields were evaluated for [Ru(bpy)₃]²⁺(PF₆⁻)₂ (Φ_{em} = 0.062) in acetonitrile as a standard (excitation wavelength was 313 nm or 365 nm). ¹H NMR spectra were measured in an acetonitrile-*d*₃ or acetone-*d*₆ solution using a JEOL AL400 (400 MHz) system. Residual protons of acetonitrile-*d*₃ and acetone-*d*₆ were used as internal standards for the measurements. The redox potentials of the complexes were measured in an acetonitrile solution containing tetraethylammonium tetrafluoroborate (0.1 M) as a supporting electrolyte by cyclic voltammetric techniques using an ALS/CHI CHI-620 electrochemical analyzer, with a glassy-carbon disk working electrode (3 mm diameter), an Ag/AgNO₃ (0.01 M) reference electrode, and a Pt counter electrode. The supporting electrolyte was dried in vacuo at 373 K for 1 day prior to use.

- (8) Sacksteder, L.; Zipp, A. P.; Brown, E. A.; Streich, L.; Demas, J. N.; DeGraff, B. A. *Inorg. Chem.* **1990**, *29*, 4335.
- (9) Walters, K. A.; Kim, Y. J.; Hupp, J. T. *Inorg. Chem.* **2002**, *41*, 2909.
- (10) Bredenbeck, J.; Helbing, J.; Hamm, P. *J. Am. Chem. Soc.* **2004**, *126*, 990.
- (11) Liard, D. J.; Busby, M.; Matousek, P.; Towrie, M.; Vlček, A., Jr. *J. Phys. Chem. A* **2004**, *108*, 2363.
- (12) Ziessel, R.; Juris, A.; Venturi, M. *Inorg. Chem.* **1998**, *37*, 5061.
- (13) (a) Koike, K.; Tanabe, J.; Toyama, S.; Tubaki, H.; Sakamoto, K.; Westwell, J. R.; Johnson, F. P.; Hori, H.; Saitoh, H.; Ishitani, O. *Inorg. Chem.* **2000**, *39*, 2777. (b) Koike, K.; Okoshi, N.; Hori, H.; Takeuchi, K.; Ishitani, O.; Tsubaki, H.; Clark, I. P.; George, M. W.; Johnson, F. P.; Turner, J. J. *J. Am. Chem. Soc.* **2002**, *124*, 11448.
- (14) (a) Wieland, S.; Reddy, K. B.; Van Eldik, R. *Organometallics* **1990**, *9*, 1802. (b) Farrell, I. R.; Vlček, A., Jr. *Coord. Chem. Rev.* **2000**, *208*, 87.
- (15) (a) Vichova, J.; Hartl, F.; Vlček, A., Jr. *J. Am. Chem. Soc.* **1992**, *114*, 10903. (b) Vlček, A., Jr.; Vichová, J.; Hartl, F. *Coord. Chem. Rev.* **1994**, *132*, 167. (c) Farrell, I. R.; Matousek, P.; Vlček, A., Jr. *J. Am. Chem. Soc.* **1999**, *121*, 5296. (d) Farrell, I. R.; Matousek, P.; Towrie, M.; Parker, A. W.; Grills, D. C.; George, M. W.; Vlček, A., Jr. *Inorg. Chem.* **2002**, *41*, 4318.
- (16) (a) Farrell, I. R.; Hartl, F.; Zalis, S.; Mahairersing, T.; Vlček, A., Jr. *J. Chem. Soc., Dalton Trans.* **2000**, 4323. (b) Farrell, I. R.; Slagereen, J. V.; Zalis, S.; Vlček, A., Jr. *Inorg. Chim. Acta.* **2001**, *315*, 44. (c) Zalis, S.; Farrell, I. R.; Vlček, A., Jr. *J. Am. Chem. Soc.* **2003**, *125*, 4580.
- (17) (a) Rosa, A.; Ricciardi, G.; Baerends, E. J.; Stufkens, D. J. *J. Phys. Chem.* **1996**, *100*, 15346. (b) Vlček, A., Jr.; Farrell, I. R.; Liard, D. J.; Matousek, P.; Towrie, M.; Parker, A. W.; Grills, D. C.; George, M. W. *J. Chem. Soc., Dalton Trans.* **2002**, 701.

Materials. Acetonitrile was dried three times over P₂O₅ and then distilled from CaH₂ prior to use. Other reagents and solvents were purchased from Kanto Chemical, Tokyo Kasei, Azmax, Wako Pure Chemical, and Aldrich and used without further purification.

The starting complexes *fac*-[Re(*bpy*)(CO)₃Cl] (**1a**), *fac*-[Re(X₂-*bpy*)(CO)₃Cl] (X₂*bpy* = 4,4'-X₂-*bpy*; X = MeO (**1b**), NH₂ (**1c**), CF₃ (**1d**)), *fac*-[Re(*bpy*)(CO)₃(pyridine)]⁺CF₃SO₃⁻ (**6**), and *fac*-[Re(*bpy*)(CO)₃(MeCN)]⁺PF₆⁻ (**7**) were synthesized according to previously reported methods.^{6,7}

Photochemical Reactions of 1a. An acetonitrile solution (500 mL) containing 230 mg (0.50 mmol) of **1a** was irradiated under an argon atmosphere using an Eikosya high-pressure Hg lamp (500 W) with a K₂CrO₄ (3.3 mM) solution filter (1 cm) until **1a** was decreased to 60% of its original concentration (about a 1.5 h irradiation). During irradiation, the reaction vessel was cooled with tap water. After the solvent was evaporated under reduced pressure, the deep red oil was chromatographed on an alumina (Merck, standardized) column using CH₂Cl₂/CH₃COOEt and then CH₂Cl₂/MeOH mixed eluents. The first fraction contained **1a**, the second contained (*OC*-6-34)-[Re(*bpy*)(CO)₂(MeCN)Cl] (**2**), and finally (*OC*-6-44)-[Re(*bpy*)(CO)₂(MeCN)Cl] (**3**) was eluted. The deep violet and deep red products **2** and **3** were recrystallized with CH₂Cl₂/ether.

(OC-6-34)-[Re(*bpy*)(CO)₂(MeCN)Cl] (2**).** Yield: 48 mg (0.101 mmol). Anal. Calcd for C₁₄H₁₁ClN₃O₂Re: C, 35.41; H, 2.33; N, 8.85. Found: C, 35.32; H, 2.13; N, 8.63. ¹H NMR (δ, 400 MHz, (CD₃)₂CO): 9.07 (d, 2H, *J* = 5.6 Hz, *bpy*-6,6'), 8.55 (d, 2H, *J* = 8.0 Hz, *bpy*-3,3'), 8.17 (dd, 2H, *J* = 8.0, 7.2 Hz, *bpy*-4,4'), 7.67 (dd, 2H, *J* = 7.2, 5.6 Hz, *bpy*-5,5'), 2.38 (s, 3H, CH₃-CN). FTIR (CH₂Cl₂): ν_{CO}/cm⁻¹ 1909, 1832.

(OC-6-44)-[Re(*bpy*)(CO)₂(MeCN)Cl] (3**).** Yield: 44 mg (0.093 mmol). Anal. Calcd for C₁₄H₁₁ClN₃O₂Re: C, 35.41; H, 2.33; N, 8.85. Found: C, 35.58; H, 2.43; N, 8.74. ¹H NMR (δ, 400 MHz, (CD₃)₂CO): 9.17 (d, 1H, *J* = 5.6 Hz, *bpy*-6), 9.02 (d, 1H, *J* = 5.6 Hz, *bpy*-6'), 8.59 (d, 1H, *J* = 8.0 Hz, *bpy*-3), 8.49 (d, 1H, *J* = 8.0 Hz, *bpy*-3'), 8.21 (dd, 1H, *J* = 8.0, 7.2 Hz, *bpy*-4), 7.99 (dd, 1H, *J* = 8.0, 7.2 Hz, *bpy*-4'), 7.69 (dd, 1H, *J* = 7.2, 5.6 Hz, *bpy*-5), 7.42 (dd, 1H, *J* = 7.2, 5.6 Hz, *bpy*-5'), 2.80 (s, 3H, CH₃-CN). FTIR (CH₂Cl₂): ν_{CO}/cm⁻¹ 1912, 1831.

(OC-6-44)-[Re(*bpy*)(CO)₂(MeCN){P(OEt)₃}]⁺PF₆⁻ (4**).** A THF solution containing 47.5 mg of **3** (0.10 mmol), 38.4 mg of TlPF₆ (0.11 mmol), and excess P(OEt)₃ was refluxed under an argon atmosphere for 15 h. After removal of precipitated TlCl by filtration, the solvent was evaporated under reduced pressure, giving red oil. Red solids were precipitated by the addition of pentane. Purification of **4** was achieved by recrystallization using CH₂Cl₂/ether.

Yield: 54 mg (0.072 mmol). Anal. Calcd for C₂₀H₂₆F₆N₃O₅P₂Re: C, 32.00; H, 3.49; N, 5.60. Found: C, 31.78; H, 3.27; N, 5.34. ¹H NMR (δ, 400 MHz, (CD₃)₂CO): 9.25 (d, 1H, *J* = 5.6 Hz, *bpy*-6), 9.20 (d, 1H, *J* = 5.6 Hz, *bpy*-6'), 8.76 (d, 1H, *J* = 8.0 Hz, *bpy*-3), 8.66 (d, 1H, *J* = 8.0 Hz, *bpy*-3'), 8.36 (dd, 1H, *J* = 8.0, 7.2 Hz, *bpy*-4), 8.15 (dd, 1H, *J* = 8.0, 7.2 Hz, *bpy*-4'), 7.84 (dd, 1H, *J* = 7.2, 5.6 Hz, *bpy*-5), 7.59 (dd, 1H, *J* = 7.2, 5.6 Hz, *bpy*-5'), 3.85 (quint, 6H, *J* = 7.0 Hz, (-CH₂-O)₃P), 2.95 (s, 3H, CH₃-CN), 1.03 (t, 9H, *J* = 7.0 Hz, CH₃-CH₂-). FTIR (CH₂Cl₂): ν_{CO}/cm⁻¹ 1959, 1876.

Photochemical Reactions of 6. An acetonitrile solution (300 mL) containing 196.2 mg (0.30 mmol) of **6** was irradiated under the same irradiation apparatus described above until **6** was decreased to 70% of its original concentration (about 6 h irradiation). After the solvent was evaporated under reduced pressure, the deep red oil was chromatographed on an alumina column with a CH₂Cl₂/CH₃COOEt mixed eluent. The first fraction contained both (*OC*-

6-44)-[Re(*bpy*)(CO)₂(pyridine)(MeCN)]⁺CF₃SO₃⁻ (**8**) and (*OC*-6-43)-[Re(*bpy*)(CO)₂(pyridine)(MeCN)]⁺CF₃SO₃⁻ (**9**). This red solution was evaporated under reduced pressure to give the deep red oil, which was chromatographed again with a silica gel (Kanto Chemical, particle size ~100–210 μm) column and CH₂Cl₂/CH₃COOEt and CH₂Cl₂/MeOH mixed eluents. The first fraction contained **9**, and the second fraction contained **8**. The red products were recrystallized with CH₂Cl₂/ether.

(OC-6-44)-[Re(*bpy*)(CO)₂(pyridine)(MeCN)]⁺CF₃SO₃⁻ (8**).** Yield: 21 mg (0.031 mmol). Anal. Calcd for C₂₀H₁₆F₃N₄O₅ReS: C, 35.98; H, 2.42; N, 8.39. Found: C, 35.98; H, 2.33; N, 8.20. ¹H NMR (δ, 400 MHz, (CD₃)₂CO): 9.34 (d, 2H, *J* = 5.2 Hz, *bpy*-6,6'), 8.70 (d, 2H, *J* = 8.0 Hz, *bpy*-3,3'), 8.60 (d, 2H, *J* = 5.2 Hz, *py*-2,6), 8.35 (dd, 2H, *J* = 8.0, 7.2 Hz, *bpy*-4,4'), 7.90 (dd, 2H, *J* = 8.0, 5.2 Hz, *py*-3,5), 7.79 (t, 1H, *J* = 8.0 Hz, *py*-4), 7.23 (dd, 2H, *J* = 7.2, 5.2 Hz, *bpy*-5,5'), 2.44 (s, 3H, CH₃-CN). FTIR (CH₂Cl₂): ν_{CO}/cm⁻¹ 1928, 1854.

(OC-6-43)-[Re(*bpy*)(CO)₂(pyridine)(MeCN)]⁺CF₃SO₃⁻ (9**).** Yield: 25 mg (0.037 mmol). Anal. Calcd for C₂₀H₁₆F₃N₄O₅ReS: C, 35.98; H, 2.42; N, 8.39. Found: C, 35.91; H, 2.28; N, 8.29. ¹H NMR (δ, 400 MHz, (CD₃)₂CO): 9.38 (d, 2H, *J* = 6.4 Hz, *bpy*-6,6'), 8.67 (d, 1H, *J* = 8.0 Hz, *bpy*-3), 8.56 (d, 1H, *J* = 8.0 Hz, *bpy*-3'), 8.46 (d, 2H, *J* = 5.2 Hz, *py*-2,6'), 8.37 (dd, 1H, *J* = 8.0, 7.2 Hz, *bpy*-4), 8.14 (dd, 1H, *J* = 8.0, 7.2 Hz, *bpy*-4'), 7.99–7.91 (m, 2H, *py*-3,5), 7.68 (t, 1H, *J* = 8.0 Hz, *py*-4), 7.41 (dd, 2H, *J* = 7.2, 6.4 Hz, *bpy*-5,5'), 2.96 (s, 3H, CH₃-CN). FTIR (CH₂Cl₂): ν_{CO}/cm⁻¹ 1932, 1854.

Photochemical Reactions of 7. An acetonitrile solution (300 mL) containing 185 mg (0.30 mmol) of **7** was irradiated under an argon atmosphere until **7** was decreased to 60% of its original concentration (about 8 h irradiation). The products **10** and **11** were obtained in a manner similar to that for **8** and **9**.

(OC-6-33)-[Re(*bpy*)(CO)₂(MeCN)₂]⁺PF₆⁻ (10**).** Yield: 17 mg (0.027 mmol). Anal. Calcd for C₁₆H₁₄F₆N₄O₂PRe: C, 30.72; H, 2.26; N, 8.96. Found: C, 30.86; H, 2.44; N, 8.93. ¹H NMR (δ, 400 MHz, (CD₃)₂CO): 9.13 (d, 2H, *J* = 5.6 Hz, *bpy*-6,6'), 8.74 (d, 2H, *J* = 8.0 Hz, *bpy*-3,3'), 8.37 (dd, 2H, *J* = 8.0, 7.2 Hz, *bpy*-4,4'), 7.86 (dd, 2H, *J* = 7.2, 5.6 Hz, *bpy*-5,5') 2.38 (s, 6H, CH₃-CN). FTIR (CH₂Cl₂): ν_{CO}/cm⁻¹ 1937, 1863.

(OC-6-32)-[Re(*bpy*)(CO)₂(MeCN)₂]⁺PF₆⁻ (11**).** Yield: 16 mg (0.026 mmol). Anal. Calcd for C₁₆H₁₄F₆N₄O₂PRe: C, 30.72; H, 2.26; N, 8.96. Found: C, 30.86; H, 2.44; N, 8.93. ¹H NMR (δ, 400 MHz, (CD₃)₂CO): 9.18 (d, 1H, *J* = 5.6 Hz, *bpy*-6), 9.15 (d, 1H, *J* = 5.6 Hz, *bpy*-6'), 8.74 (d, 1H, *J* = 8.1 Hz, *bpy*-3), 8.65 (d, 1H, *J* = 8.1 Hz, *bpy*-3'), 8.39 (dd, 1H, *J* = 8.1, 7.2 Hz, *bpy*-4), 8.19 (dd, 1H, *J* = 8.1, 7.2 Hz, *bpy*-4'), 7.87 (dd, 1H, *J* = 7.2, 5.6 Hz, *bpy*-5), 7.62 (dd, 1H, *J* = 7.2, 5.6 Hz, *bpy*-5'), 2.88 (s, 3H, CH₃-CN) 2.28 (s, 3H, CH₃-CN). FTIR (CH₂Cl₂): ν_{CO}/cm⁻¹ 1940, 1866.

Crystal Structure Determination. The crystals were grown from CH₂Cl₂/pentane for **2** and from acetonitrile/ether for **4** with the vapor-diffusion technique, and intensity data were collected on a Rigaku R-AXIS RAPID diffractometer with an IP detector using Mo Kα radiation (λ = 0.71073 Å). The images were interpreted and integrated with the program PROCESS-AUTO (Automatic data acquisition and processing package for imaging plate diffractometer, Rigaku Corp., Tokyo, Japan, 1998). Both structures were solved by direct methods using TEXSAN (program for the crystal structure; M.S.C. Corp., The Woodlands, TX, 2000) and refined on *F*² by means of full-matrix least-square procedures, using SHELXL97 (program for crystal refinement; G. M. Sheldrick, University of Göttingen, Göttingen, Germany, 1997). Non-H atoms were refined anisotropically, and the riding mode was used for H atoms with

isotropic temperature factors fixed to be 1.2 times the $U(\text{eq})$ of the parent atoms (1.5 times for methyl groups).

Crystal data for 2: $\text{C}_{14}\text{H}_{10}\text{ClN}_3\text{O}_2\text{Re}$, $M = 473.90$, triclinic, $P2_1/n$, $a = 8.1712(6)$ Å, $b = 12.1173(13)$ Å, $c = 16.3830(11)$ Å, $\beta = 100.369(2)^\circ$, $V = 1595.6(2)$ Å³, $Z = 4$, $D_c = 1.973$ g cm⁻³, μ (Mo K α) = 7.788 mm⁻¹, $F(000) = 892$, $T = 293$ K, crystal size = 0.15 mm \times 0.07 mm \times 0.05 mm, 3612 independent reflections ($R_{\text{int}} = 0.041$), final $R1 = 0.0315$ for 3184 reflections with $I > 2\sigma(I)$ and $wR2 = 0.0727$ for all data.

Crystal data for 4: $\text{C}_{20}\text{H}_{26}\text{F}_6\text{N}_3\text{O}_5\text{P}_2\text{Re}\cdot 0.35\text{H}_2\text{O}$, $M = 750.58$, triclinic, $P\bar{1}$, $a = 13.881(15)$ Å, $b = 13.202(17)$ Å, $c = 8.397(9)$ Å, $\alpha = 108.65(4)^\circ$, $\beta = 72.22(3)^\circ$, $\gamma = 103.68(4)^\circ$, $V = 1372(3)$ Å³, $Z = 2$, $D_c = 1.817$ g cm⁻³, μ (Mo K α) = 4.621 mm⁻¹, $F(000) = 732$, $T = 273$ K, crystal size = 0.20 mm \times 0.16 mm \times 0.04 mm, 6091 independent reflections ($R_{\text{int}} = 0.025$), final $R1 = 0.0488$ for 5488 reflections with $I > 2\sigma(I)$ and $wR2 = 0.1628$ for all data.

Quantum Yield Measurements of the Photochemical Reactions. For measurements of rates and quantum yields of the photochemical reactions, an Ushio 500 W high-pressure Hg lamp for 313 and 365 nm light or an Ushio 500 W Xe lamp for 290, 300, 313, and 330 nm light was employed with band-pass filters supplied from Asahi-Bunko (half-bandwidth is 10 nm). A gentle stream of argon was bubbled into a solution containing the complex (1.0 mM) for 15 min, and the solution was then photolyzed. For determination of the quantum yields, irradiation was stopped before **1a** decreased up to 10% to avoid inner filter effects by the products. Under this condition, the concentration of the starting complexes decreased linearly with the irradiation time (Supporting Information, Figure S1). The temperature of the solution was controlled within ± 0.1 °C by using an IWAKI CTS-134A cooling thermopump during irradiation. The reaction solutions were kept at room temperature in the dark for 2 h after irradiation and then analyzed using the HPLC procedure described above. The irradiation light intensities were determined using a $\text{K}_3\text{Fe}(\text{C}_2\text{O}_4)_3$ or acetone chemical actinometer.¹⁸

TRIR Measurements. Picosecond time-resolved IR (TRIR) spectra were obtained using the equipment and procedures described previously.^{17,19,20} In short, the sample solution was excited (pumped) at 266 nm, obtained by mixing the 800 nm fundamental and frequency-doubled 400 nm pulses of a Ti:sapphire laser of ~ 150 fs duration (fwhm), ~ 2 μJ per pulse. TRIR spectra were probed at selected time delays with IR (~ 150 fs) pulses obtained by difference-frequency generation. The IR probe pulses cover a spectral range ca. 200 cm⁻¹ wide and are tunable from 1000 to 5000 cm⁻¹. The diameter of the pump and probe laser pulses was 150–200 μm . The spectra were investigated in the region of ν_{CO} vibrations with resolutions of 4–5 cm⁻¹ per experimental point. The measurements were performed on sample solutions flowing through a 0.25 mm CaF_2 IR cell, which was raster-scanned to prevent localized laser heating and photochemical decomposition. TRIR spectra in the nanosecond time domain were measured using the same detection instrument. An electronically synchronized Nd:YAG laser producing 1 ns, 267 nm pulses was used for pumping.²¹ All spectral and kinetic fitting was performed using Microcal Origin 7 software.

- (18) (a) Murov, S. L.; Carmichael, I.; Hug, G. L. *Handbook of Photochemistry*, 2nd ed.; Marcel Dekker, Inc.: New York, 1993. (b) Hatchard, C. G.; Parker, C. A. *Proc. R. Soc. London, Ser. A* **1956**, 235, 518. (c) Haim, A.; Sutin, N. *J. Am. Chem. Soc.* **1965**, 20, 4211. (19) Liard, D. J.; Busby, M.; Farrell, I. R.; Matousek, P.; Towrie, M.; Vlček, A., Jr. *J. Phys. Chem. A* **2004**, 108, 556. (20) Towrie, M.; Grills, D. C.; Dyer, J.; Weinstein, J. A.; Matousek, P.; Barton, R.; Bailey, P. D.; Subramaniam, N.; Kwok, W. M.; Ma, C. S.; Phillips, D.; Parker, A. W.; George, M. W. *Appl. Spectrosc.* **2003**, 57, 367.

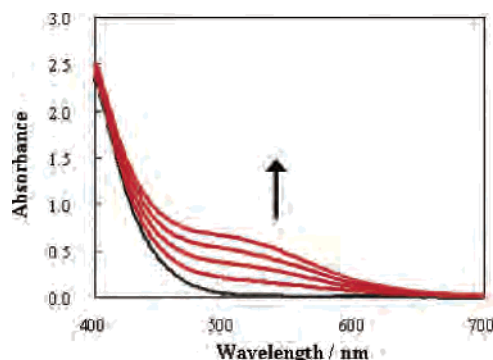


Figure 1. UV-vis absorption spectral change in an acetone nitrile solution containing 0.2 mM of **1a** under an argon atmosphere monitored in situ during irradiation by using 313 nm light at 298 K (interval 20 min).

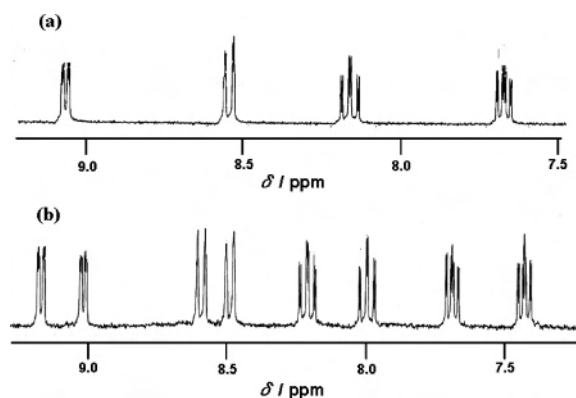


Figure 2. Aromatic proton peaks in ¹H NMR spectra of **2** (a) and **3** (b) in acetone-*d*₆ solutions.

Results and Discussion

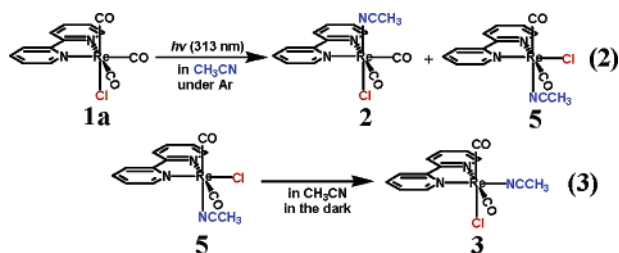
Photochemical Reactions and Products. An acetone nitrile solution containing 0.2 mM **1a** was irradiated using 313 nm light under an argon atmosphere. During irradiation, the UV-vis absorption spectrum changed, as shown in Figure 1.

From the reaction solution, the two products of **2** and **3** were isolated in yields of 28 and 26% (based on **1a** consumed), respectively, by column chromatography. Elemental analyses and ESI-MS data using the Na⁺ addition method²² indicate that **2** and **3** have the same component, i.e., $[\text{Re}(\text{bpy})(\text{CO})_2(\text{MeCN})\text{Cl}]$. On the other hand, the ¹H NMR spectra of these complexes were different, as shown in Figure 2: four aromatic protons were observed for **2**, but eight were observed for **3**. These results clearly show that **2** and **3** are geometrical isomers of each other. X-ray crystallographic analysis was successfully performed for **2** (Figure 3a). The complex **2** has two carbonyl ligands in the trans positions to the bpy ligand; the acetonitrile and chloro ligands coordinate to the central rhenium in trans positions to each other (eqs 2 and 3); i.e., the structure of **2** is (OC-6-34)- $[\text{Re}(\text{bpy})(\text{CO})_2(\text{MeCN})\text{Cl}]$.

Correspondingly, **3** should have a cis,cis structure, with carbonyl ligands set respectively in cis and trans positions

- (21) Towrie, M.; Parker, A. W.; Vlček, A., Jr.; Gabrielson, A.; Blanco Rodriguez, A. M. *Appl. Spectrosc.* **2005**, 59, 467.

- (22) Hori, H.; Koike, K.; Ishizuka, M.; Westwell, J. R.; Takeuchi, K.; Ibusuki, T.; Ishitani, O. *Chromatographia* **1996**, 43, 491.



to the *bpy* ligand, since there is no symmetry plane between the two pyridine rings of the *bpy* ligand. There are two possible structures: in one, the chloro and the acetonitrile ligands are respectively located in the trans and cis positions to the *bpy* ligand, and the second is the reverse of this. Suitable crystals of **3** for X-ray crystallography could not be obtained, and instead, **3** was converted to **4** by reaction with TlPF₆ and P(OEt)₃, which was isolated in 72% yield. X-ray crystallographic analysis was performed for **4** as shown in Figure 3b: the acetonitrile ligand is in the trans position to the *bpy* ligand, and P(OEt)₃ is in the cis position, i.e., (OC-6-44)-[Re(*bpy*)(CO)₂(MeCN){P(OEt)₃}]⁺PF₆⁻. As expected, its ¹H NMR spectra showed eight aromatic protons, and the chemical shift of the methyl protons in the acetonitrile ligand of **4** was almost the same as that in **3**. Concrete identification of **3** is described later.

Table 1 summarizes selected bond distances and angles of **2** and **4**, which are similar to those reported for other *fac*-rhenium(I) diimine tricarbonyl complexes²³ and *cis,trans*-[Re(*bpy*)(CO)₂(PPh₃){P(OEt)₃}]⁺,¹³ except for the smaller angle of C–Re–NCMe in **2**.

The reaction solutions were analyzed using HPLC with an ODS column. Figure 4 shows (a) chromatograms of a reaction solution immediately after 1.5 h of irradiation and (b) the same solution after an additional 2 h, kept at room temperature in the dark. These chromatograms show that the three products of **2**, **3**, and **5** are present immediately after irradiation, whereas **5** is slowly but quantitatively converted to **3** in the dark. Since a short period of irradiation produced only a small amount of **3** compared with **2** and **5** (Supporting Information, Figure S2), we conclude that **1a** is converted photochemically to **2** and **5**, and further dark reaction of **5** then produces **3** (eq 3). The disappearance quantum yield of **1a** was determined as 0.01 ± 0.001 using 313 nm monochromatic light at 298 K. HPLC analysis of reaction solutions kept in dim light for 2 h after irradiation also showed that the combined yield of **2** and **3** was greater than 27% of the initial concentration of **1a** when 30% of **1a** had been consumed, but further irradiation lowered the yield because of photodecomposition of the products (Supporting Information, Figure S3).

Although the product **5** could not be isolated because of its instability, quick measurements of the reaction solution just after irradiation provided ¹H NMR (Figure 5), IR (Figure 6), UV–vis (Supporting Information, Figure S4), and liquid

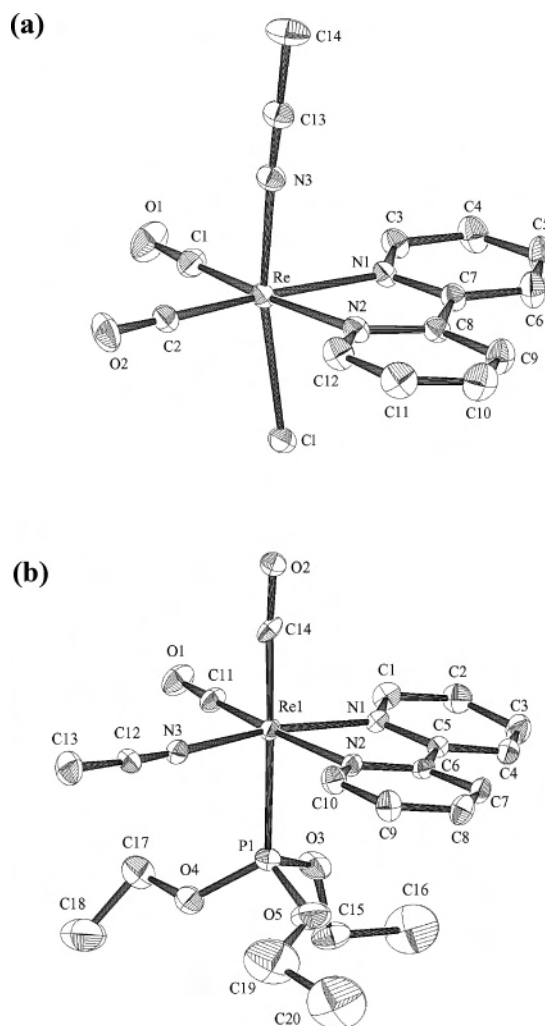


Figure 3. ORTEP drawing of (a) **2** and (b) **4**. Displacement ellipsoids are shown at the 20% probability level. H atoms and a counteranion are omitted for clarity. CCDC-279829 (**2**) and CCDC-279683 (**4**).

chromatography mass spectra of **5**. This complex is another isomer of **2** and **3** and has eight aromatic protons corresponding to its *bpy* ligand. The IR and ¹H NMR data of **5** are summarized with those of **2** and **3** in Table 2. The proton peak in the 6-position on the *bpy* ligand of **5** (9.62 ppm) was observed in a magnetic field to be about 0.5 ppm lower than those of **3** (9.13 ppm) and **4** (9.25 ppm). A similar downfield shift has been reported in the case of Ru *bpy* complexes, in which a Cl ligand lies at the trans position to the *bpy* ligand, being caused by a CH/*n* interaction (*n* refers to lone pair electrons in Cl).²⁴ The logical conclusion is that the Cl ligand is in the cis position to the *bpy* ligand in **3** as well as **4**. The structure of **5** then is (OC-6-24)-[Re(*bpy*)(CO)₂(MeCN)Cl], with the Cl ligand located in the trans position to the *bpy* ligand (eq 3). The Cl ligand must therefore flip from the cis position to the *bpy* ligand to the trans position during the formation of **5**.²⁵ The isomerization of **5** to **3** probably proceeds without breaking a bond, because

(23) (a) Belanger, S.; Hupp, J. T.; Stern, C. L. *Acta Crystallogr.* **1998**, C54, 1596. (b) Haddad, S. F.; Marshall, J. A.; Crosby, G. A.; Twamley, B. *Acta Crystallogr.* **2002**, E58, m559. (c) Shaver, R. J.; Perkovsky, M. W.; Rillema, D. P.; Woods, C. *Inorg. Chem.* **1995**, 34, 5446.

(24) Gerli, A.; Reedijk, J.; Lakin, M. T.; Spek, A. L. *Inorg. Chem.* **1995**, 34, 1836.

(25) A similar phenomenon has been reported in the photochemistry of the Mn complex *fac*-[Mn(Pr-DAB)(CO)₃Br] (Pr-DAB = *N,N'*-diisopropyl-1,4-diaza-1,3-butadiene). See reference 17.

Table 1. Selected Bond Lengths (Å) and Angles (deg) for **2** and **4**

2, Bond Lengths							
Re–C(1)	1.881(5)	Re–C(2)	1.876(4)	Re–N(3)	2.043(4)	Re–Cl	2.467(10)
Re–N(1)	2.190(3)	Re–N(2)	2.181(3)	C(1)–O(1)	1.164(6)	C(2)–O(2)	1.163(5)
2, Bond Angles							
C(2)–Re–C(1)	86.7(2)	C(1)–Re–N(1)	99.95(18)	C(1)–Re–Cl	95.37(14)	C(2)–Re–N(1)	173.38(16)
C(1)–Re–N(2)	174.29(18)	C(1)–Re–N(3)	93.63(17)	C(2)–Re–N(2)	99.03(17)	C(2)–Re–N(3)	91.92(17)
C(2)–Re–Cl	95.15(13)	N(2)–Re–N(1)	74.36(12)	N(3)–Re–N(2)	85.73(13)	N(2)–Re–Cl	84.66(9)
N(3)–Re–N(1)	87.89(13)	N(1)–Re–Cl	84.09(9)	N(3)–Re–Cl	168.85(10)		
4, Bond Lengths							
Re–C(11)	1.878(10)	Re–C(14)	1.881(10)	Re–N(3)	2.097(10)	Re–P(1)	2.424(4)
Re–N(1)	2.126(8)	Re–N(2)	2.189(8)	C(11)–O(1)	1.176(12)	C(14)–O(2)	1.223(12)
4, Bond Angles							
C(11)–Re–C(14)	90.1(4)	C(11)–Re–N(1)	96.4(4)	C(1)–Re–P(1)	90.0(3)	C(14)–Re–N(1)	95.0(4)
C(11)–Re–N(2)	171.1(4)	C(11)–Re–N(3)	95.6(4)	C(14)–Re–N(2)	92.4(3)	C(14)–Re–N(3)	88.6(4)
C(14)–Re–P(1)	178.4(3)	N(2)–Re–N(1)	74.9(3)	N(3)–Re–N(2)	93.0(3)	N(2)–Re–P(1)	87.8(2)
N(3)–Re–N(1)	167.5(3)	N(1)–Re–P(1)	86.5(2)	N(3)–Re–P(1)	89.8(3)		

the addition of a large excess $\text{P}(\text{OEt})_3$ to the reaction solution just after irradiation did not retard the formation of **3**, and complexes with a $\text{P}(\text{OEt})_3$ ligand, such as $[\text{Re}(\text{bpy})(\text{CO})_2\{\text{P}(\text{OEt})_3\}\text{Cl}]$, were not detected. The $\text{C}=\text{O}$ stretching bands of **5** were observed a few wavenumbers lower than those of **3** (Figure 6), and the MLCT absorption band of **5** is red-shifted compared with that of **3** (Supporting Information, Figure S4).

PLS Reactions of Other Rhenium Complexes. It should be noted that PLS reactions take place also for other rhenium(I) diimine tricarbonyl complexes $\text{fac}[\text{Re}(\text{X}_2\text{bpy})(\text{CO})_3\text{Cl}]$ ($\text{X}_2\text{bpy} = 4,4'\text{-X}_2\text{-bpy}$; $\text{X} = \text{MeO}$ (**1b**), NH_2 (**1c**), CF_3 (**1d**)), $\text{fac}[\text{Re}(\text{bpy})(\text{CO})_3(\text{pyridine})]^+\text{CF}_3\text{SO}_3^-$ (**6**), and $\text{fac}[\text{Re}(\text{bpy})(\text{CO})_3(\text{MeCN})]^+\text{PF}_6^-$ (**7**), giving the corresponding *cis-cis* and *cis,trans*-rhenium(I) dicarbonyl complexes. The disappearance quantum yields of the starting complexes using 313 nm monochromatic light were 0.009 ± 0.001 for **1b**, 0.020 ± 0.003 for **1c**, 0.002 for **1d**, 0.005 for **6**, and 0.002 for **7** at 298 K. The products, (*OC*-6-44)- and (*OC*-6-43)- $[\text{Re}(\text{bpy})(\text{CO})_2(\text{MeCN})(\text{pyridine})]^+\text{CF}_3\text{SO}_3^-$ (**8** and **9**), and (*OC*-6-32)- and (*OC*-6-33)- $[\text{Re}(\text{bpy})(\text{CO})_2(\text{MeCN})_2]^+\text{PF}_6^-$ (**10** and **11**), were isolated in yields of 10–16% based on the starting

complex consumed (Scheme 1). To our knowledge, *cis,cis*-rhenium(I) dicarbonyl complexes **3**, **4**, **9**, and **11** have not yet been reported before,²⁶ and **2**, **8**, and **10** are the first isolated *cis,trans*-rhenium(I) diimine dicarbonyl complexes without a phosphorus ligand.¹³ Their spectral and electrochemical data are summarized in Table 3.

Properties of New Dicarbonyl Rhenium(I) Complexes.

UV–vis absorption spectra and cyclic voltammograms of both **2** and **3** are shown as typical examples. Figure 7 shows the UV–vis absorption spectra of **2** and **3** measured in MeCN and in CH_2Cl_2 . The two broad bands at 480–525 and 350–380 nm are the characteristic features, distinct from *fac*- $[\text{Re}(\text{bpy})(\text{CO})_3(\text{L})]^n+$ and $[\text{Re}(\text{bpy})(\text{CO})_2(\text{PR}_3)(\text{L})]^n+$ complexes, which show a MLCT absorption band at much shorter wavelength (350–420 nm). Because a red shift of both absorption bands (10–30 nm) was observed on changing

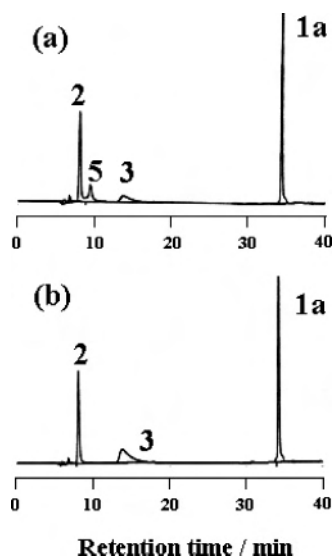


Figure 4. HPLC chromatograms of the photoreaction solution containing **1a** (1.0 mM) (a) immediately after 1.5 h irradiation and (b) after the irradiated solution has been kept at room temperature in the dark for 2 h.

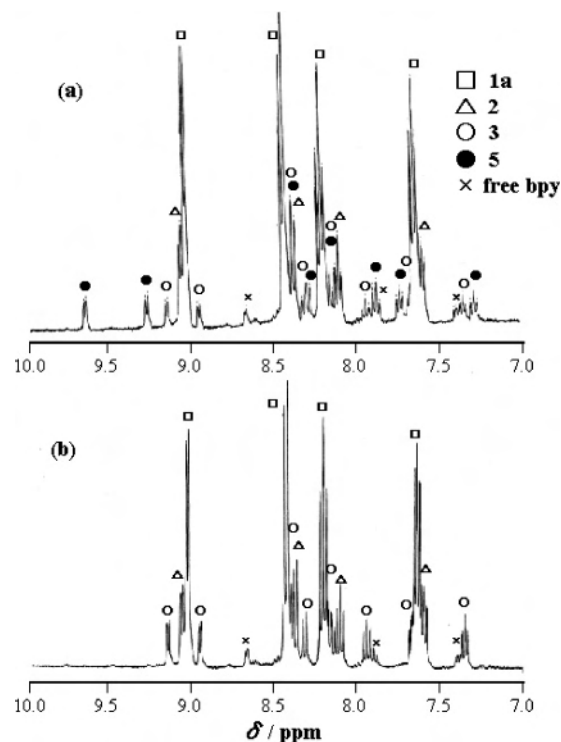


Figure 5. ^1H NMR spectra of an irradiated CD_3CN solution containing **1a** (1.0 mM) (a) just after 0.5 h irradiation and (b) after being kept at room temperature in the dark for 2 h after irradiation.

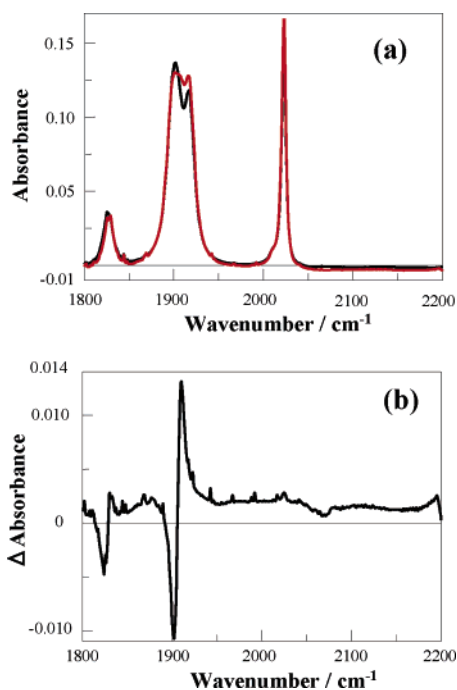


Figure 6. (a) IR spectra of an irradiated MeCN solution containing **1a** (0.5 mM) (black) immediately after 1 h irradiation and (red) after being kept at room temperature in the dark for 1 h after irradiation. (b) Differential spectrum of the red spectrum from the black.

Table 2. IR and ¹H NMR Spectral Data of **1a**, **2**, **3**, and **5**

complex	¹ H NMR/ppm in CD ₃ CN					IR/cm ⁻¹ in MeCN
	bpy-6	bpy-3	bpy-4	bpy-5		
1a	9.02	8.43	8.20	7.63		2023, 1917, 1899
2	9.05	8.38	8.08	7.58		1906, 1828
3	9.13, 8.94	8.41, 8.32	8.15, 7.93	7.67, 7.34		1909, 1828
5^a	9.62, 9.25	8.39, 8.30	8.14, 7.89	7.72, 7.28		~1902, ~1824

^a Obtained by using Figures 5 and 6.

the solvent from MeCN to CH₂Cl₂, these bands should be attributed to the first and second Re^I → (bpy) MLCT transitions.⁹ The other band around 300 nm is attributable to a π–π*(bpy) transition. The cyclic voltammograms of **2** and **3** are illustrated in Figure 8. Interestingly, both first-reduction (bpy/bpy^{•-}) and first-oxidation (Re^I/Re^{II}) waves are reversible, in contrast to those of most reported rhenium(I) diimine complexes *fac*-[Re(LL)(CO)₃]ⁿ⁺ and *cis,trans*-[Re(LL)(CO)₂(PR₃)(L)]⁺, which show at least one irreversible wave. Two CO stretching bands in both IR spectra of **2** and **3** were observed with similar strengths at similar wavenumbers (Supporting Information, Figure S5).

In all cases, the MLCT absorption bands of the *cis,cis* isomer were observed at 10–35 nm longer wavelengths

compared with those of the corresponding *cis,trans* isomer. Although MLCT absorption energy of many transition-metal diimine (LL) complexes shows good correlation with the “redox energy” [$E_{1/2}^{\text{ox}}(\text{M}^{n+}/\text{M}^{(n+1)}) - E_{1/2}^{\text{red}}(\text{LL}/\text{LL}^{\bullet-})$], this is not the case of the *cis,trans* and *cis,cis* isomers; see Table 3. The oxidation $E_{1/2}^{\text{ox}}$ of the *cis,cis* isomers was more negative than that of the corresponding *cis,trans* isomers, whereas the first-reduction wave of both complexes occurs at similar potentials.^{27,28} However, the MLCT absorption of the *cis,cis* isomers was observed at a 10–35 nm longer wavelength than that of the *cis,trans* isomer.

Reaction Mechanism. Mechanistic studies provide new insight into the photochemical and photophysical peculiarities of the rhenium(I) diimine complexes, as follows:

(1) The PLS reaction rate of **1a** was not affected by the presence of O₂, but emission of **1a** was efficiently quenched with the rate constant of $3.6 \times 10^9 \text{ M}^{-1} \text{ s}^{-1}$ by O₂, indicating that PLS does not occur from the emissive state.

(2) Figure 9 shows the UV–vis absorption spectra of the starting complexes **1a** and **1b** together with the excitation-wavelength dependence of the quantum yields of the PLS reaction. Irradiation into the lower energy part of the lowest ¹MLCT absorption band, typically using 365 nm light, did not cause any PLS reaction. The onset of the PLS reaction is seen at about 330 nm, in the blue side of the lowest absorption band. The quantum yield then sharply increases with decreasing irradiation wavelength. It follows that PLS requires excitation to upper electronic excited states and/or higher vibrational levels of the lowest ¹MLCT state.

(3) The quantum yield Φ_{em} of the emission of **1c** slightly decreases with decreasing irradiation wavelength: the values of 0.0145 ± 0.0003 and 0.0129 ± 0.0002 were determined using 365 and 313 nm excitation wavelengths, respectively. This result clearly shows that higher excited states of **1c** undergo an ultrafast process that is competitive with the population of the lowest ³MLCT state. The quantum yield of ³MLCT formation is thus less than unity. The quantum yield of the population of the nonemissive and, probably, reactive state can be calculated as about 0.11 using the difference of Φ_{em} between 365 and 313 nm excitations.

(4) TRIR spectra of the complexes **1a** and **1c** were measured following UV excitation with 266 nm, ~150 fs laser pulses on a time scale ranging from 1 ps to 100 μs. The spectrum of **1a** (Figure 10) measured at the earliest time delays after excitation (1–5 ps) shows negative “bleach” bands due to depletion of the ground-state population, strong up-shifted bands due to the lowest ³MLCT state at 1952 and

Table 3. Spectral and Electrochemical Data of Isolated [Re(*bpy*)(CO)₂(L)(L’)]ⁿ⁺

complex		λ_{max} (ε)/nm (M ⁻¹ cm ⁻¹) ^a					V vs Ag/AgNO ₃ ^b		
no.	structure	L	L’	MLCT(1)	MLCT(2)	IR ^a /cm ⁻¹	$E_{1/2}^{\text{ox}}$	$E_{1/2}^{\text{red}}$	$E_{\text{p}}^{\text{red}}$
2	<i>cis,trans</i>	MeCN	Cl	515 (3000)	360 (3500)	1909, 1832	0.09(65)	-1.81(60)	-2.36
3	<i>cis,cis</i>	MeCN	Cl	525 (2800)	380 (3500)	1912, 1830	0.30(65)	-1.82(55)	-2.18
8	<i>cis,trans</i>	MeCN	py	440 (3800)	~350 (sh)	1937, 1863	0.62(65)	-1.66(65)	-2.08
9	<i>cis,cis</i>	MeCN	py	475 (3800)	365 (4200)	1940, 1866	0.65(65)	-1.68(65)	-2.03
10	<i>cis,trans</i>	MeCN	MeCN	465 (3800)	~350 (sh)	1928, 1854	0.57(70)	-1.62(70)	-2.16
11	<i>cis,cis</i>	MeCN	MeCN	500 (3300)	365 (6900)	1932, 1854	0.61(70)	-1.64(65)	-2.08

^a Measured in CH₂Cl₂. ^b Measured in MeCN.

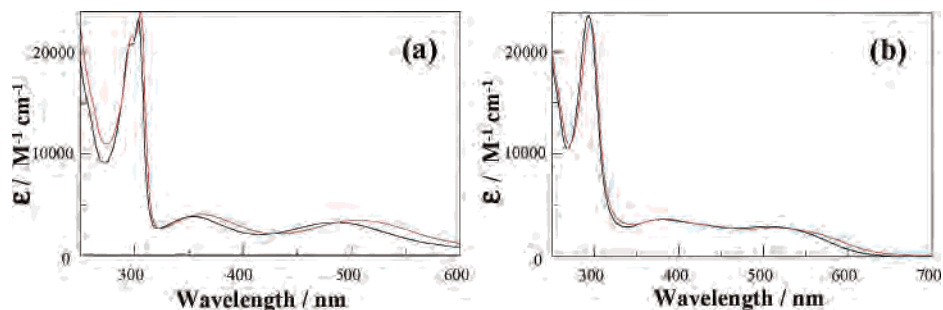


Figure 7. UV-vis absorption spectra of (a) **2** and (b) **3** measured in acetonitrile (black) and CH_2Cl_2 (red) solutions at 298 K.

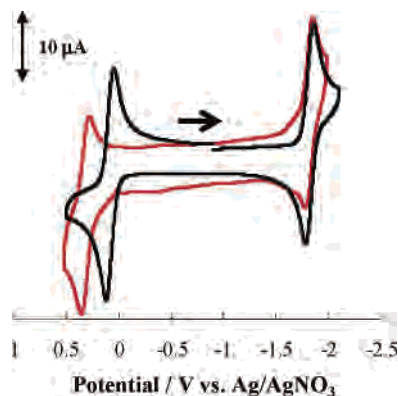


Figure 8. Cyclic voltammograms of **2** (black) and **3** (red) measured in acetonitrile solutions containing tetraethylammonium tetrafluoroborate (0.1 M) using a glassy-carbon working electrode, a Pt counter electrode, and a Ag/AgNO_3 (0.01 M) reference electrode. The scan rates were 200 mV/s.

1986 cm^{-1} , and a weak broad absorption in the low-wavenumber region, extending from $\sim 1860\text{ cm}^{-1}$ to the end of the spectral window investigated, ca. 1770 cm^{-1} . By 10 ps, this broad absorption decreases and a distinct weak band at $\sim 1824\text{ cm}^{-1}$, with a small shoulder at $\sim 1819\text{ cm}^{-1}$ emerges. It slightly narrows and grows in intensity until 50–100 ps. The formation time can be roughly estimated as 30 ps (Supporting Information, Figure S6). Within experimental accuracy, the 1824 cm^{-1} band can be attributed to the dicarbonyl photoproducts. On a longer time scale, the $^3\text{MLCT}$ features and the bleach bands decay, while the 1824 cm^{-1} band stays nearly constant and another product band emerges at 1900 cm^{-1} , which at shorter time delays was hidden by the overlapping bleach (Figure 11). This experiment proves that the photoproduct is not formed from the $^3\text{MLCT}$ state. The TRIR spectra of **1c** are very similar (Supporting Information, Figures S7 and S8). The photoproduct band, seen at about 1805 cm^{-1} , is slightly more intense than that in the **1a** spectrum, in accordance with the higher PLS quantum yield.

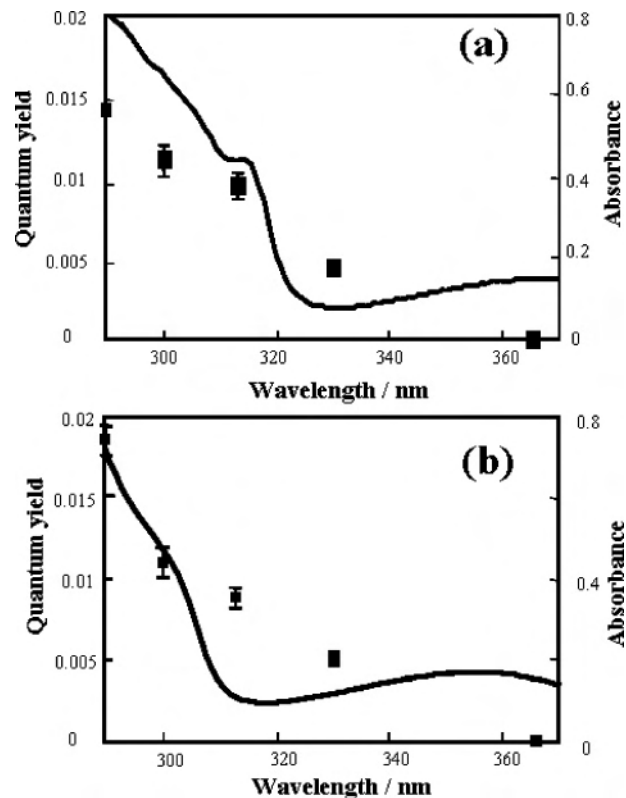


Figure 9. UV-vis absorption spectra (solid line) of (a) **1a** and (b) **1b** and dependence of PLS quantum yields on the excitation wavelength (plots with an error bar).

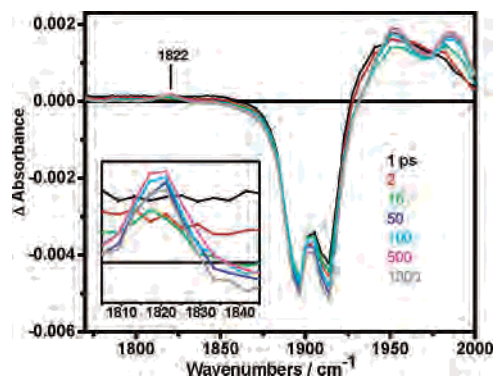


Figure 10. Picosecond-difference TRIR spectra of **1a** in MeCN measured at selected time delays after 266 nm, ~ 150 fs excitation with a Ti:S laser. Experimental points are separated by 4–5 cm^{-1} . Inset: Expansion of the low-wavenumber region showing the formation of the photoproduct band.

To summarize, the CO dissociation of **1a** and **1c** produces **2** and **5** with subpicosecond rates, following UV excitation. The photoproducts are vibrationally highly excited (“hot”),

- (26) A few *cis*-rhenium(I) dicarbonyl complexes with two bidentate ligands were reported: (a) Schutte, E.; Helms, J.; Woessner, S.; Bowen, J.; Sullivan, B. P. *Inorg. Chem.* **1998**, *37*, 2618. (b) Smithback, J. L.; Helms, J. B.; Schutte, E.; Woessner, S. M.; Sullivan, B. P. *Inorg. Chem.* **2006**, *45*, 2163.
- (27) (a) Baiano, J. A.; Kessler, R. J.; Lumpkin, R. S.; Munley, M. J.; Murphy, W. R., Jr. *J. Phys. Chem.* **1995**, *99*, 17680. (b) Baiano, J. A.; Carlson, D. L.; Wolosh, G. M.; DeJesus, D., E.; Knowles, C. F.; Szabo, E. G.; Murphy, W. R., Jr. *Inorg. Chem.* **1990**, *29*, 2327. (c) Baiano, J. A.; Murphy, W. R., Jr. *Inorg. Chem.* **1991**, *30*, 4594. (d) Feliz, M. R.; R.-Nieto, F.; Ruitz, G.; Wolcan, E. *J. Photochem. Photobiol., A* **1998**, *117*, 185.
- (28) Juris, A.; Barigelletti, F.; von Zelewsky, A.; Balzani, V. *Inorg. Chem.* **1986**, *25*, 256.

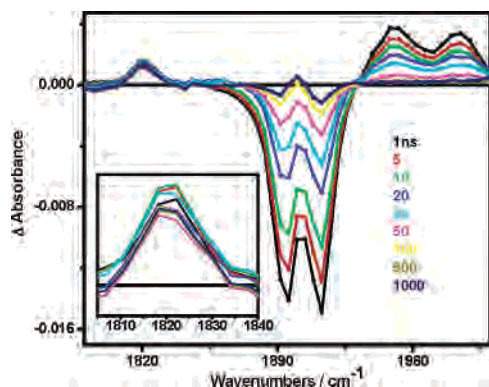


Figure 11. Nanosecond-difference TRIR spectra of **1a** in MeCN measured at selected time delays after 267 nm, ~ 1 ns excitation with a Nd:YAG laser. (Note that the product accumulation occurs during the laser pulse.) Experimental points are separated by $4\text{--}5\text{ cm}^{-1}$. Inset: Expansion of the low-wavenumber region showing the photoproduct band.

as documented by the very broad IR absorption that is present already at 1 ps after excitation. Vibrational relaxation of the photoproduct, which occurs on a picosecond time scale, is manifested by conversion of the broad “backgroundlike” absorption into a distinct photoproduct band. Similar picosecond growth of photoproduct bands from a very broad IR absorption has been seen before for CO-loss photoproducts, radicals, or triplet states formed upon laser-pulse excitation of various metal carbonyls.^{29–35} The optically populated upper electronic excited states of **1a** and **1c** decay by (at least) two competitive femtosecond processes: intersystem crossing into the lowest ³MLCT state and prompt CO dissociation. The relevant optically populated state(s) can be of Re \rightarrow bpy, Re \rightarrow CO MLCT, or intraligand (bpy) origin. Some of them can be inherently dissociative with respect to the Re–CO bond whereas others can acquire a dissociative character through interaction (avoided crossing) with higher repulsive states, either MC or Re \rightarrow CO MLCT.^{36–39} Formation of the final products from the reactive state(s) should compete with the recovering processes of the starting complex such as nonradiative decay and recombination.⁴⁰ In the case of **1c**, the ratio between formation of the products and recovery of **1c** can be calculated as about 2:9 at 298 K by using the formation quantum yields of the

products (2%) and of the nonemissive state(s) ($\sim 11\%$), which can be estimated from the data described in the mechanistic investigation no. 3. Such a prompt CO dissociation is similar to that of a prototypical complex [Cr(CO)₄(bpy)],¹⁵ with one important exception: the chromium complex reacts from its lowest optically populated Cr \rightarrow bpy ¹MLCT state, whereas the lowest Re \rightarrow bpy ¹MLCT state is unreactive and the photochemistry requires higher electronic excitation. Prompt M–CO dissociation from metal carbonyl–diimine complexes is usually attributed to an interaction between optically populated ¹MLCT state(s) and dissociative MC states along the reaction coordinate, that is, the Re–CO elongation.^{15,35–38,41–43} Strong avoided crossing then makes the ¹-MLCT potential energy surface repulsive with respect to the M–CO bond. For the third-row transition-metal Re, the energy of the relevant MC state can be supposed to be much higher and to drop with the Re–CO bond elongation much more slowly than in the case of Cr. Hence, the avoided crossing in Re complexes occurs at higher energies, requiring excitation above the lowest MLCT absorption band. Another contributing factor could be the higher Re–CO dissociation energy. For both complexes, the photochemical quantum yield is essentially determined by the branching ratio of the evolution of the optically prepared state between CO dissociation and relaxation to the lowest triplet state, ³MLCT. The mechanistic studies show that this emissive ³MLCT state does not undergo the PLS reaction.

Conclusion

We have reported that the PLS reactions of *fac*-[Re(bpy)-(CO)₃Cl] and its derivatives are caused by high-energy light, such as that of 313 nm wavelength. The mechanistic studies including TRIR measurements clearly show that the PLS reactions do not proceed via the lowest ³MLCT excited state but, instead, via higher vibrational levels of the ¹MLCT state and/or higher electronic excited state(s) such as ¹ $\pi\text{--}\pi^*$ and the higher-lying Re \rightarrow bpy and Re \rightarrow CO ¹MLCT states. The CO dissociation is a subpicosecond process producing highly excited CO-loss product. Relaxed photoproduct forms during 50–100 ps after excitation. This PLS reaction is more general, occurring for various *fac*-rhenium(I) diimine tricarbonyl complexes, and is therefore potentially applicable as a general synthetic method of novel types of *cis,cis*- and *cis*-*trans*-rhenium(I) diimine dicarbonyl complexes.

Acknowledgment. This work was partly supported by Grant-in-Aid for Scientific Research Nos. 18350029 and 18033014 from the Ministry of Education, Culture, Sports, Science and Technology of Japan. Mike Towrie and Kate Ronayne of the CCLRC Rutherford Appleton Laboratory (U.K.) are thanked for their help with measurement of the TRIR spectra.

Supporting Information Available: X-ray crystallographic files in CIF format; Figure S1, decrease of **1a** in the first stage of the

- (29) Asbury, J. B.; Ghosh, H. N.; Yeston, J. S.; Bergman, R. G.; Lian, T. *Organometallics* **1998**, *17*, 3417.
 (30) Asbury, J. B.; Hang, K.; Yeston, J. S.; Cordaro, J. G.; Bergman, R. G.; Lian, T. *J. Am. Chem. Soc.* **2000**, *122*, 12870.
 (31) Dougherty, T. P.; Heilweil, E. J. *J. Chem. Phys.* **1994**, *100*, 4006.
 (32) Snee, P. T.; Payne, C. K.; Kotz, K. T.; Yang, H.; Harris, C. B. *J. Am. Chem. Soc.* **2001**, *123*, 2255.
 (33) Yang, H.; Snee, P. T.; Kotz, K. T.; Payne, C. K.; Harris, C. B. *J. Am. Chem. Soc.* **2001**, *123*, 4204.
 (34) Asplund, M. C.; Snee, P. T.; Yeston, J. S.; Wilkens, M. J.; Payne, C. K.; Yang, H.; Kotz, K. T.; Frei, H.; Bergman, R. G.; Harris, C. B. *J. Am. Chem. Soc.* **2002**, *124*, 10605.
 (35) Portius, P.; Yang, J.; Sun, X. Z.; Grills, D. C.; Matousek, P.; Parker, A. W.; Towrie, M.; George, M. W. *J. Am. Chem. Soc.* **2004**, *126*, 10713.
 (36) Vlček, A., Jr. *Coord. Chem. Rev.* **1998**, *177*, 219.
 (37) Goumans, T. P. M.; Ehlers, A. W.; van Hemert, M. C.; Rosa, A.; Baerends, E. J.; Lammertsma, K. *J. Am. Chem. Soc.* **2003**, *125*, 3558.
 (38) Baerends, E. J.; Rosa, A. *Coord. Chem. Rev.* **1998**, *177*, 97.
 (39) Pollak, C.; Rosa, A.; Baerends, E. J. *J. Am. Chem. Soc.* **1997**, *119*, 7324.
 (40) Lian, T.; Bromberg, S. E.; Asplund, M. C.; Yang, H.; Harris, C. B. *J. Phys. Chem.* **1996**, *100*, 11994.

- (41) Farrell, I. R.; Matousek, P.; Towrie, M.; Parker, A. W.; Grills, D. C.; George, M. W.; Vlček, A., Jr. *Inorg. Chem.* **2002**, *41*, 4318.
 (42) Vlček, A. Jr. *Coord. Chem. Rev.* **2002**, *230*, 225.
 (43) Guillaumont, D.; Daniel, C.; Vlček, A., Jr. *J. Phys. Chem. A* **2001**, *105*, 1107.

photochemical reaction; Figures S2 and S3, time–conversion curves of the photoproducts; Figure S4, UV–vis absorption spectral change of **5**; Figure S5, IR spectra of **2** and **3**; Figure S6, time profile of the intensity of the photoproduct band; Figures S7 and S8,

picosecond-difference TRIR spectra of **1c** in MeCN. This material is available free of charge via the Internet at <http://pubs.acs.org>.

IC0621603